Reconstruction of ultrasonic wavefronts from the field of the circular transducer

E.Jasiûnienë, L.Maþeika

Prof. K.Barðauskas Ultrasound Research Center

Kaunas University of Technology

Introduction

The purpose of the ultrasonic reflection tomography is to construct from the reflection data a quantitative cross-sectional image displaying a distribution of the specific ultrasonic parameter in the material under a test. A simple filtered backprojection method along circular arcs is usually used to obtain reconstructed images [1-3]. The reconstructed images are imperfect because of ultrasound wavefront curvature. In order to achieve better resolution of reconstructed images in the ultrasound reflection tomography , the curvature of the wavefronts has to be known and taken into account performing backprojection.

Reconstruction of wavefronts of pulsed ultrasound fields is very complicated, because amplitude and phase of a wave are not constant and varies in all directions. The pulsed wave fields were extensively theoretically and experimentally studied by J.P.Weight and *et al.* [4-6]. These studies showed, that assuming idealized piston source, experimental results are in good agreement with theoretical results.

The goal of our work was to develop wavefront reconstruction algorithm of ultrasonic fields, radiated by sources of finite dimensions and for circular transducer to test usually in the ultrasonic reflection tomography used assumption, that wavefronts are spherical [1-3].

Theory of wave propagation

The wave, propagating in three dimensions, can be written [7]:

$$u(x, y, z, t) = \left(A_x \vec{i} + A_y \vec{j} + A_z \vec{k} \right) \cos\left(k_x x + k_y y + k_z z - \omega t \right)$$

(1)

where u is the disturbance in space at the position x, y, z and time t; A_{xi}, A_{yj}, A_{zk} are the amplitudes of the components of the disturbance in the x, y and z directions; k_x, k_y, k_z are the components of the wave vector in three dimensions, ω is the angular frequency.

Usually it is assumed, that wavefront is location in space with equal phase, e.g. a particular pressure amplitude. So the equation of a wave can be written as a constant value of the phase:

1.Equation of a plane wave can be expressed:

$$k_x x + k_y y + k_z z - \omega t = \phi .$$ (2)

2.Equation of spherical wave can be expressed:

$$k_r r - \omega t = \phi ,\tag{3}$$

where r is the radial distance from the origin; k_r is the wave vector in a radial direction.

Ultrasonic beams, radiated by sources of finite dimensions, diverge and for this reason ideal plane waves can not be excited. An energy, radiated by a transducer, does not remain in the cylinder, the base of which is the piston, but after some distance, called near field zone, spreads into the cone.

A near field zone can be expressed [7]:

$$N = \frac{s}{\pi \lambda} ,\tag{4}$$

where $s = \pi R^2$ is the area of the transducer, R is the transducer radius, $\lambda = c/f$ is the wavelength, c is the ultrasound velocity, f is the frequency of the transducer.

This spreading reduces the intensity of the wave. The approximate picture of the beam spreading is presented in Fig.1. An actual beam divergence process is much more complex.

The pulsed field of the transducer can be calculated using the mathematical model based on the spatial impulse response approach [8]. The spatial impulse response of the disk with radius R is given by the following expressions:

$$h_t(x,y,z,t) =$$

$$\begin{cases} -\rho_0 c \delta(t - t_0), & x < R, \quad t_0 \le t \le t_1 \\ -\dfrac{\rho_0 c}{\pi} \dfrac{d\theta}{dt} & x \ne R, \quad t_1 \le t \le t_2 \\ -\rho_0 c \left[\delta(t - t_0) + \dfrac{1}{\pi} \dfrac{d\theta_1}{dt} \right] & x = R, \quad t_0 \le t \le t_2 \end{cases}$$

$$(5)$$

where

$$\frac{d\theta}{dt} = -\left[c^2 t \left(c^2 t^2 - y^2 - x^2 + R^2 \right) \right] / \left(c^2 t^2 - y^2 \right)$$

$$\times \sqrt{ \left[2\left(c^2 t^2 - y^2\right)\left(x^2 + R^2\right) - \left(c^2 t^2 - y^2\right)^2 - \left(x^2 - R^2\right)^2 \right] }$$

$$\frac{d\theta_1}{dt} = -\frac{c^2 t}{\sqrt{\left(c^2 t^2 - y^2\right)\left[4R^2 - \left(c^2 t^2 - y^2\right)\right]}} ,\tag{6}$$

$$t_0 = y/c,$$

$$t_1 = \sqrt{(R-x)^2 + y^2} / c,\tag{7}$$

$$t_2 = \sqrt{(R+x)^2 + y^2} / c .$$

The structure of the pulsed field can be explained using concept of direct plane and edge waves. The whole surface of a piston generates a direct plane wave, which propagates in cylindrical region having the piston at its base. From edge of the transducer diffracted edge waves are radiated, which propagate in all directions from the edge of the piston.

Algorithm for calculation of wavefronts coordinates

The detailed explanation of the wavefront calculation algorithm is given in [9], and only brief description of it is included here.

A transmitter radiates an impulse into space, and the time of flight t_f of the impulse from transmitter to receiver is measured. Usually it is assumed, that a wavefront is location of points with an equal phase. In the case of pulsed ultrasonic fields we can assume, that wavefront is location in space which is reached by the wave after the same time t_c.

So, when the time of flight from a transmitter to a receiver t_f is measured, and the time of flight from the transmitter to the particular wavefront t_c is known, we can calculate the distance from the receiver to the wavefront (Fig.2.):

$$a_{tf} = \left(t_f - t_c \right) c ,\tag{8}$$

where t_f is the measured time of flight; t_c is the time of flight when receiver is in front of the transmitter, c is the velocity of ultrasound in the medium.

The exact curvature of the wavefront is not known, so we don't known how to backproject calculated distance from the receiver to the wavefront. This distance can be backprojected in all directions along the radius of the circle, the center coordinates of which are coordinates of the receiver, and radius is equal to the distance from the receiver to the wavefront a_{tf} calculated according (8).

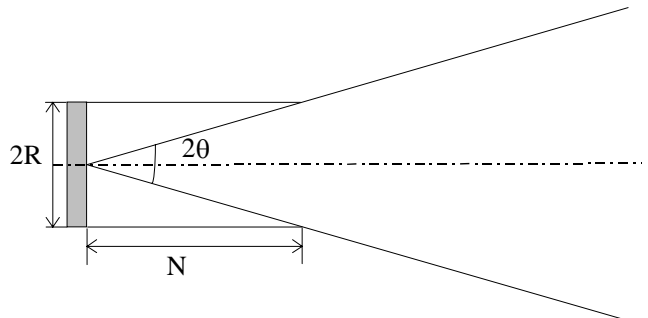We had developed two methods for a calculation of ultrasonic wavefronts coordinates, using two different

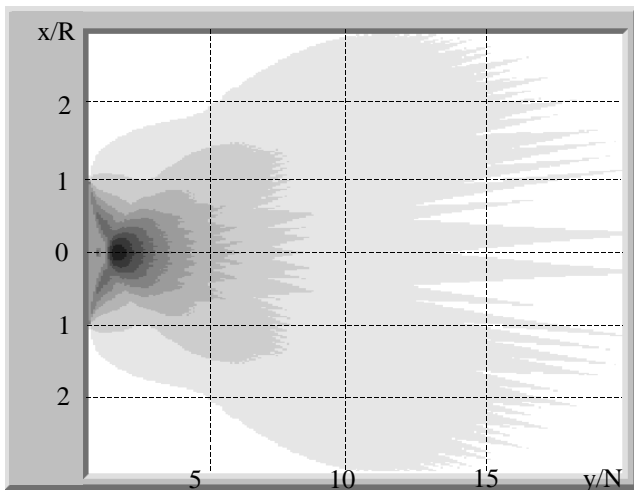Fig.1. **Beam spreading diagram**

assumptions:

Fig.3. **The field of the transducer in the zone y=0÷20N, x=-3R÷3R.**

1.**Spherical wave approach method.** We assume the transducer to be a point type transducer, which radiates spherical waves into space. The coordinates of the wavefront can be found backprojecting the distance from the receiver to the wavefront along the radius from the transmitter to the receiver (Fig.2):

$$x_{fs} = x_r - a_{tf} \sin\alpha,$$
$$y_{fs} = y_r - a_{tf} \cos\alpha. \tag{9}$$

2.**Plane wave approach.** We assume the transducer to be plane wave transducer, which radiates plane waves into space. Then the coordinates of the wavefront can be found backprojecting the distance from the receiver to the wavefront along lines from the receivers, parallel to the axis of the
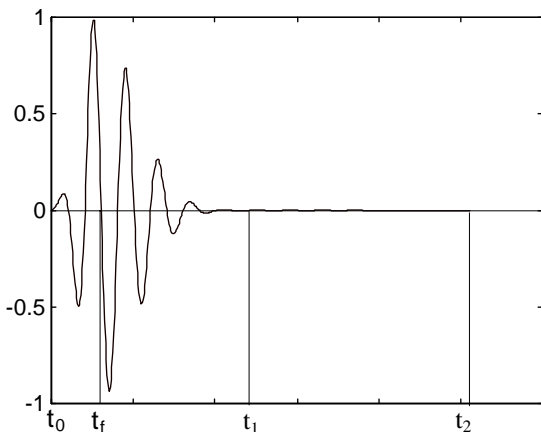

Fig.5. **Zero- crossing technique**

transmitter (Fig.2):

$$x_{fp} = x_r,$$
$$y_{fp} = y_r - a_{tf}. \tag{10}$$
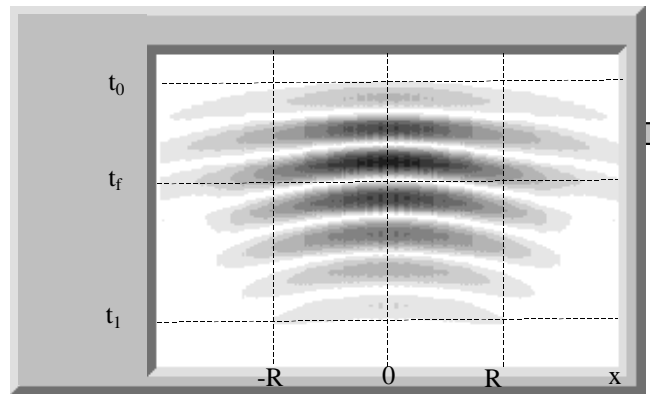

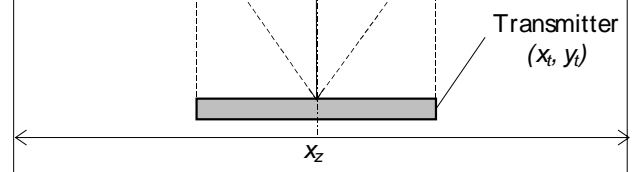Fig.6. **B-scan image of the transducer field.**

Fig.2. **Reconstruction of ultrasonic wavefronts**

Computation results

Field radiated by a circular transducer was calculated. Then, using previously described methods, wavefronts at various distances from the transducer were reconstructed. The calculations were performed for a wideband disk type transducer of the radius R=7mm and with the center frequency f=2.5MHz. It was assumed, that transducer radiates radiopulse with the Gaussian envelope, duration of which was two periods.

The field of the transducer was calculated in the zone y=0÷20N, x=-3÷3R. In the Fig.3 whole computed field is presented, and in Fig.4 the field in the zone y=0÷3N, x=-2R÷2R is presented.

The time of flight was evaluated using the signal zero-crossing technique (Fig.5.). It means, that the time of flight t_f was measured, after signal reaches maximum and then changes a sign from positive to negative. B-scan image of the field of the transducer, is presented in Fig.6.

The reconstructed wavefronts were compared with two types of hypothetical wavefronts:

• wavefront of a point transducer - spherical wavefront (SW) (Fig.7);

• ideal wavefront of a circular transducer - combi-nation of plane and spherical wavefronts (CW) (Fig.8).

The wavefronts were reconstructed at various distances from the transducer: y=0.5N (Fig.9); y=N (Fig.10); y=2N (Fig.11); y=3N (Fig.12); y=5N (Fig.13).
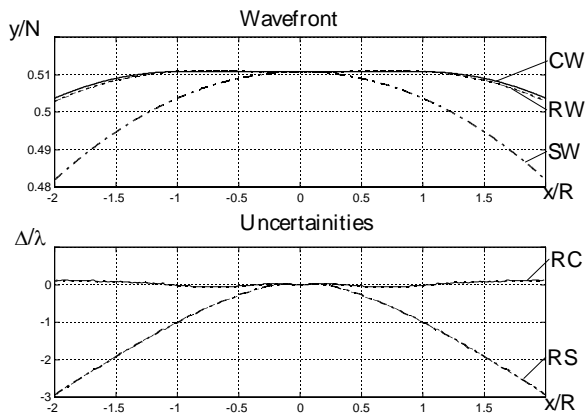
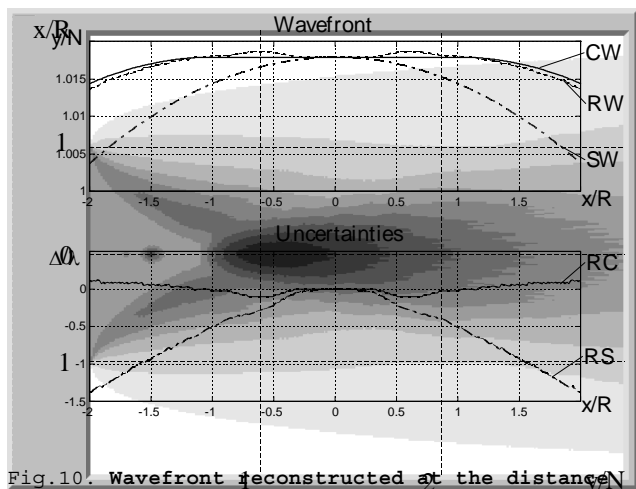Fig.9. **Wavefront reconstructed at the distance y=0.5N from the transducer and corresponding uncertainities**

Fig.10. **Wavefront reconstructed at the distance y=N from the transducer and corresponding uncertainities**
Fig.4. **The field of the transducer in the zone y=0÷3N, x=-2R÷2R.**
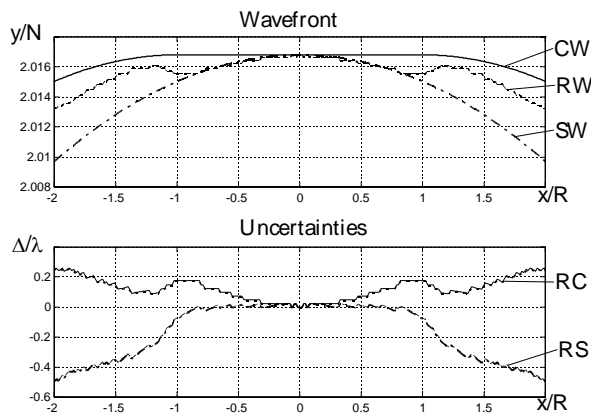

Fig.11. **Wavefront, reconstructed at the distance y=2N from the transducer and corresponding uncertainities**

Reconstructed wavefronts in the figures are marked as RW. Uncertainty between the reconstructed wavefront and the spherical wavefront in the figures is marked as RS, and uncertainty between reconstructed wavefront and the

ideal wavefront of a circular transducer is marked as RC.

As can be seen from the results presented in Fig.9 and Fig.10., in the near field zone, that is, when $y \leq N$, the wavefront is the combination of plane and spherical wavefronts. Due to the edge waves the wavefronts are not ideally plane within the geometrical beam region in the near field zone (the uncertainty $RC < 0.1\lambda$). Outside geometrical beam region the wavefront corresponds to the spherical wave, radiated by the edges of the transducer.

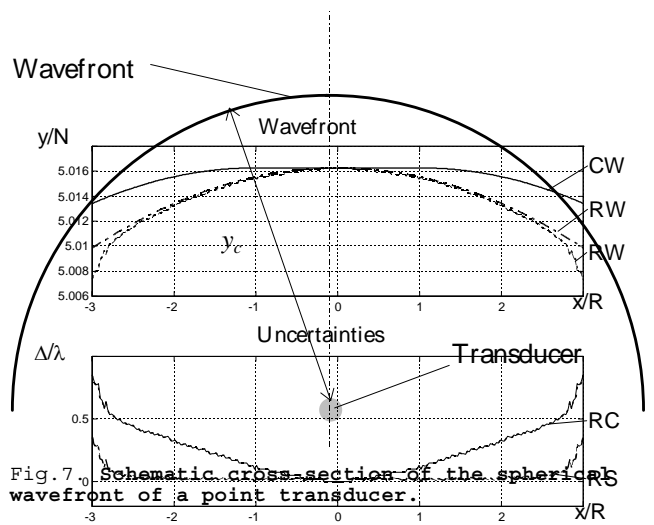When $N < y \leq 3N$ (Fig.11. and Fig.12.),

Fig.7. **Schematic cross-section of the spherical wavefront of a point transducer.**

Fig.12. **Wavefront reconstructed at the distance y=5N from the transducer and corresponding uncertainities**
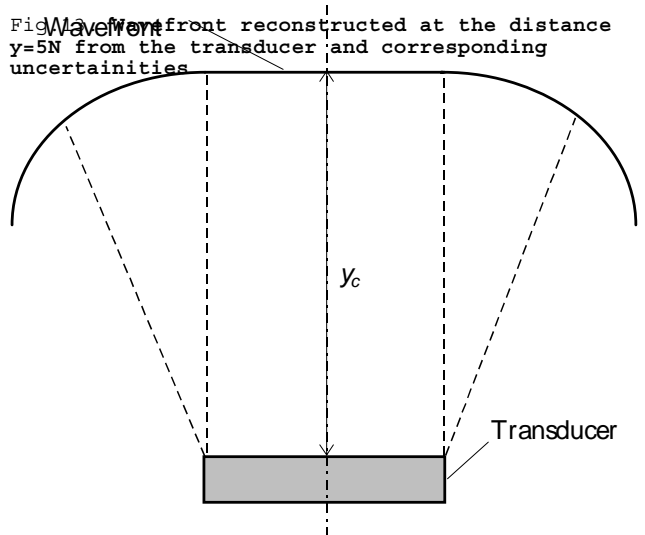

Fig.8. **Schematic cross-section of the wavefront of a circular transducer**

we have an intermediate zone. In the geometrical beam region wavefronts can be assumed to be spherical with the uncertainty $RS < 0.01\lambda$, but outside the geometrical beam region it is not possible to approximate them by simple curves with a small uncertainty.

In the far field zone (Fig.13), that is, when $y > 3N$, calculated wavefronts are in a good agreement with spherical wavefronts. So, with the uncertainty $RS < 0.05\lambda$, we can assume, that transducer is a point type transducer and it is transmitting a spherical wave. On the sides of the zone errors are bigger, because the amplitude of the signal is small and errors can be due to the fact, that zeros of the pulsed signal are not correctly found.

Conclusions

New method for a reconstruction of wavefronts of ultrasonic waves from data collected at discrete points in a fixed plane, perpendicular to a propagation direction, has been proposed. The accuracy of the method was determined comparing the reconstructed wavefronts with those obtained theoretically from a model of the baffled piston type circular transducer.

From the results presented it is seen, that shape of the wavefront depends on the distance between the wavefront and a transmitter. The computed wavefronts can be analyzed in terms of plane and edge waves radiated:

1. In the near field zone, $y \leq N$, with uncertainty less than 0.1λ, wavefronts can be assumed to be the combination of the plane and spherical wavefronts.

2. In the intermediate zone $N < y < 3N$, in the geometrical beam region, wavefronts can be assumed to be spherical. Outside the geometrical beam region, due to edge waves, form of the wavefront becomes complex, and it can not be approximated to simple curves.

3. In the far field zone, $y > 3N$, with uncertainty less than 0.05λ, wavefronts can be assumed to be spherical wavefronts.

Acknowledgments

References

1. **Sponheim N. and Johansen I**. ''Experimental Results in Ultrasonic Tomography Using a Filtered Backpropagation Algorithm'', Ultrasonic Imaging, vol.13, pp.56-70. 1991.
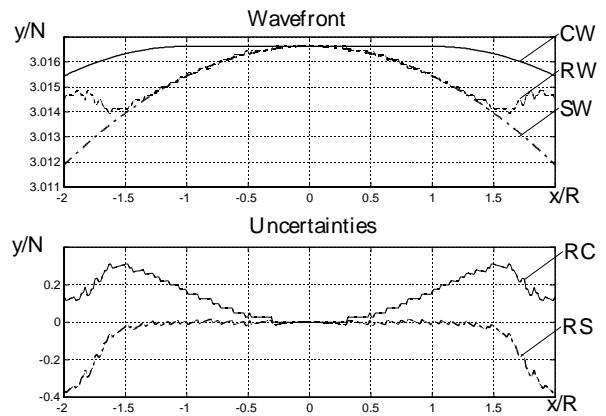2. **Moshfeghi M. and Hanstead P.D.** ''Ultrasound reflection tomography of cylindrical rods'', Ultrasonics, pp.206-214. 1985.
3. **Jasiûnienë E., Maþeika L., Ðliteris R.** ''Experimental results in ultrasound reflection tomography for nondestructive testing'', Ultragarsas, Nr.1(26), pp.7-11. 1996.
4. **Weight J.P., Hayman A.J.** ''Observations of the propagation of very short ultrasonic pulses and their reflection by small targets'', J. Acoust. Soc. Am., vol.63, No.2, pp.396-404. 1978.
5. **Hayman A.J., Weight J.P.** ''Transmission and reception of short ultrasonic pulses by circular and square transducers'', J. Acoust. Soc. Am., vol.66, No.4, pp.945-951. 1979.
6. **Weight J.P.** ''Ultrasonic beam structures in fluid media'', J. Acoust. Soc. Am., vol.76, No.4, pp.1184-1191. 1984.
7. Nondestructive Testing Handbook, 2nd edition, vol.7., Ultrasonic Testing/ Albert S.Birks, Robert E. Green, Paul McIntire.- USA: American Society for Nondestructive Testing, 1991.
8. **Robinson D.E.** ''Near field transient radiation patterns for circular pistons'', IEEE Trans. Acoust. Speech Sign. Proc. ASSP-22, pp.395-405. 1974.
9. **Jasiûnienë E.** ''Reconstruction of ultrasonic wavefronts'', Matavimai, No.2, 1997. (accepted for a publication).

Fig.12. **Wavefront reconstructed at the distance y=3N from the transducer and corresponding uncertainities**

E.Jasiûnienë, L.Maþeika

Ultragarsiniø bangø frontø atkûrimas ið apskritojo keitiklio lauko

Reziumë

Bangos frontams atkurti ið apskritojo ultragarsinio keitiklio lauko naudotasi nauju metodu. Nustatyta, kad artimojoje zonoje, kai $y \leq N$, su neapibrëþtimi 0.1λ gali bûti laikoma, kad bangos frontai yra plokðèiø ir sferiniø bangø kombinacija. Tolimojoje zonoje, kai $y > 3N$, su neapibrëþtimi 0.05λ gali bûti laikoma, kad bangos frontai yra sferiniai. Tarpinëje zonoje, kai $N < y < 3N$, geometrinio spindulio ribose bangos frontai yra sferiniai, o uþ geometrinio spindulio ribø jie negali bûti aproksimuoti paprastomis kreivëmis.